HeDI: Healthcare Device Interoperability for IoT-Based e-Health Platforms

Nidhi Pathak, *Student Member, IEEE,* Sudip Misra, *Senior Member, IEEE,* Anandarup Mukherjee, *Student Member, IEEE,* and Neeraj Kumar, *Senior Member, IEEE*

Abstract—In this work, we propose and develop HeDI (<u>He</u>althcare <u>D</u>evice <u>I</u>nteroperability) – a system to enable device interoperability in IoT-enabled in-home healthcare monitoring platforms. The system consists of multiple sensors, each connected wirelessly to an edge device, acting as a wireless communication gateway to a remote server. The system initiates information handshaking between the sensor adapters and edge device at the beginning of the operation, which is later used to detect the sensor settings to process the data received from the sensor. The system is scalable and dynamically accommodates multiple sensors without any predefined ontologies at the edge device. The implementation of our system avoids dependencies on a system's physical ports. The low form factor and wireless connectivity of the adapter make the system portable and convenient for in-home health monitoring. Additionally, the system allows multiple homogeneous sensors to operate at the same time in the same system. We implement and evaluate our system with a 3-lead ECG, pulse, and temperature sensors against two different network configurations – Star and Mesh. We use the data set generated from our implemented system for performance analysis. The network-level analysis of our system shows an average packet delivery ratio of 0.92 for star network configuration and 0.98 for mesh network configuration, ensuring the reliability of performance and its suitability for healthcare monitoring systems.

Index Terms—Interoperability, Interoperable adapter, IoT, in-home health monitoring, e-Health, Edge platforms.

I. INTRODUCTION

THE inability to share data among different systems drastically reduces the efficiency and limits the functionality of the IoT environment [1]. Interoperability has emerged as a robust enabler of cross-domain communication [2]. Traditional IoT-based device discovery protocols are based on predefined device profiles. They require real-time installation of device drivers, in addition to being heavy for resource and energy-constrained IoT devices. The available plug-and-play solutions for IoT devices such as [3], [4] are lightweight and versatile but require supporting drivers. The availability of these drivers is subject to their availability in the system repository or online access by these IoT devices. Traditionally, wireless health sensors have been designed in such a manner that each wearable unit consists of a fixed number of heterogeneous sensors. Considering S_n to be the set of standalone sensor units such that $S_n = \{s_1, s_2, s_3, \cdots, s_n\}, n \in \mathbb{Z}^+$ are

N. Pathak is with the Advanced Technology Development Center at Indian Institute of Technology Kharagpur, India

S. Misra and A. Mukherjee are with the Department of Computer Science and Engineering at Indian Institute of Technology Kharagpur, India

N. Kumar is with the Department of Computer Science and Engineering at Thapar Institute of Engineering & Technology, India

connected/wired to a wearable unit G_T, which also acts as its communication gateway. Additionally, considering S_t be
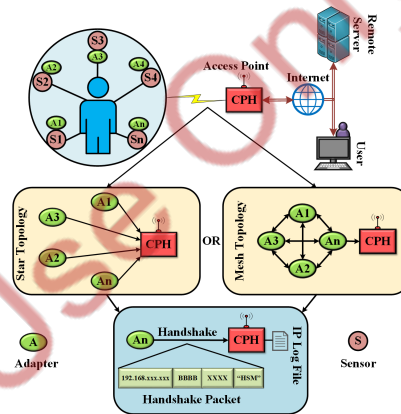

Fig. 1: Network architecture of the implemented system

the set of possible sensor types supported by the healthcare system, $S_t = \{\gamma_1, \gamma_2, \gamma_3, \cdots, \gamma_m\}, m \in \mathbb{Z}^+$. The set of sensors S that can communicate to G_T is represented by the following relation,

$$S \subseteq S_n \times S_t, \ \forall (s_i, \gamma_j)_{i,j=1:n} \in S,$$
$$s_i \mid_{i=1:n} \in S_n, \text{ and } \gamma_j \mid_{j=1:n} \in S_t \tag{1}$$

The cardinality of S from the relation in Equation (1) is $|S| = |S_n \times S_t| = n \times m$. However, in the currently available remote healthcare monitoring systems, each of the sensors attached to G_T is designed to be unique, such that $i = j$ and

$$\forall (s, \gamma) \in S_n$$
$$f(s) = f(\gamma) \implies s = \gamma \tag{2}$$

The cardinality of the configuration of S from the relation in Equation (2) is $|S| = |S_n| = |S_t| = n$. This denotes the limited number of sensor combinations, which are possible using the currently available remote health monitoring units.

In this work, we propose and implement HeDI – a framework for in-home remote health monitoring, which consists of interoperable sensor adapters ($A = \{A_1, A_2, \cdots, A_n\}$), a processing hub/gateway (G_T), and a remote server. Fig. 1 shows the network architecture of our proposed system. Each adapter connects its sensor to the processing hub for the collection of heterogeneous physiological data from a human body. The collected data is forwarded to the remote server. HeDI can be scaled up for multiple adapters and processing gateways in a network. Fig. 2 shows the interconnection

between multiple components of HeDI. The adapters and processing hubs are connected to the remote server through the Internet. The figure shows mode of communication, range of operation and the estimated number of connected devices. Each of these adapters is interoperable in the sense that it
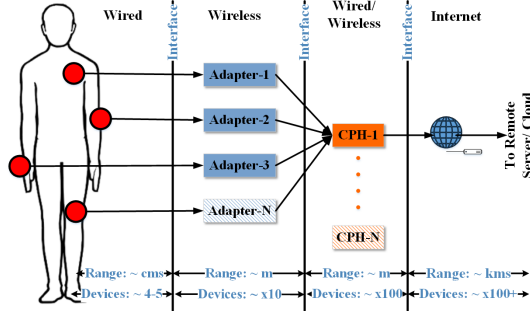

Fig. 2: An overview of a scaled up version of HeDI.

requires no specific port for its connection to the system. Any new sensor with the proposed interoperable sensor adapter connects to an existing system without making any physical changes to the processing hub or the remote server. This feature allows us to achieve the relational mapping outlined in Equation (1), such that the number of supported sensors and sensor type combinations are significantly larger than the ones currently available in the market. HeDI addresses the challenge of device interoperability through an IP-based mapping scheme. The IP-based mapping keeps a record of the connected sensor of an adapter and its corresponding IP address to process the incoming data. Additionally, the IP-based mapping also allows the system to have multiple homogeneous sensors to connect to the system simultaneously, such that $|W| = |S_n|$ where W is the set of wearable adapters. Considering the set of sensor types to be S_t, the relation denoting the number of adapters that can communicate to G_T is similar to the relation in Equation (1), with a cardinality of $|W \times S_t|$.

As the system is used in remote healthcare monitoring, it is expected that the system and the ensuing network have maximum accuracy and minimum delays. We evaluate our system for two different network configurations – star and mesh. Each sensor adapter in the star configuration connects directly to a Central Processing Hub (CPH). This arrangement enables the sensor to send data directly to CPH without the help of any intermediate adapters and minimizes the delays. In the case of the mesh network, the sensor adapters form a network among themselves, whenever they are in range, and broadcast their data to the network, ensuring that there is no loss of information. However, the mesh configuration increases redundant data in the network and is limited by network delays. Both configurations have a trade-off between the accuracy and delay, which we try to analyze for our implementation.

A. Motivation

The challenge of interoperability has been taken up in multiple domains to exchange data among heterogeneous platforms and devices. Edge-centric solutions have been proposed to enable context and protocol interoperabilities [5]. Interoperability among different platforms has been proposed using semantic extractions, vocabularies, data fusion [6] [6]. The solutions mainly focus on the aspect of data processing, post data collection. The existing solutions require predefined devices, systems, and architectures to support interoperability. The feature of scalability and flexibility of device integration still needs to be addressed with a real solution to it. Our system primarily aims to provide a scalable and flexible solution capable of integrating resource-constrained IoT devices without making any physical changes to the existing system.

B. Research Challenges

The proposed system uses wireless communication with multiple sensor nodes forming a network of devices. We outline the primary research challenges of our work below:

- **Wireless Communication:** Multiple wearable sensors have to be wirelessly connected to CPH. The system and its communication channel should support wearable devices and data transmission with high accuracy and efficiency.
- **Interoperability:** The wearable sensors have to be integrated into the system without any predefined information. This implies that the CPH or the server should be capable of identifying the data received from a wearable. This is addressed using an IP-based mapping scheme, discussed in later sections.
- **Sensor failure:** The current proposal offers a reusable sensor adapter to be used as a wearable. In case of any sensor malfunction, the sensor can easily be replaced with a new one and attached to the same adapter. This replacement does not affect the other adapters, the CPH, or the system as a whole. Further, if the adapter experiences any fault, the adapter can be simply replaced with a new one, without requiring any changes to the other adapters or the system as a whole. This feature also helps in keeping the long-term maintenance cost of the system to a minimum.
- **Interference:** In the case of multiple access points present in the range of the adapters, the system may suffer from frequent disconnections from the CPH due to interference from other wireless network devices if they are using the same channel. The issue can be avoided by using alternative communication technology such as Bluetooth to connect the wearables to the CPH

C. Contributions

Existing IoT-based health monitoring approaches provide constrained, non-scalable solutions to provide interoperability to a system. These approaches use semantic ontologies, following standards, and cross-domain platforms. Our implemented system enables interoperability among different health sensors connected to a system. Our developed devices are not predefined in the system and integrate dynamically without any prior information. The contributions of this work are as follows:

- We propose and implement IP-based interoperability in an in-home remote healthcare monitoring system. The system is independent of any predefined ontologies.
- We implement an interoperable sensor adapter to connect multiple heterogeneous health monitoring sensors. The sensor adapter enables the integration of different sensors to the system dynamically and makes the system modular.
- We implement a fully functional system with the proposed architecture and algorithms. We analyze the system along with its network characterization for two network configurations – star and mesh, to study the reliability and accuracy of the system while ensuring its scalability.

II. RELATED WORKS

Health monitoring devices allow continuous monitoring of physiological conditions through emotion cognition, chronic illness, and elderly patients [7] [8]. Intelligent fabrics such as [9] and devices such as [10] are designed to monitor the physical and psychological health along with the surrounding. The exchange of information between these devices and systems helps to analyze a patient's overall health. We limit our discussion to the existing approaches to enable interoperability and identify the current requirements.

Platform based interoperability allows different systems and platforms to communicate with each other by acting as a middleware. Sigwele *et al.* [11] conceptualized a collaborative platform to allow semantic interoperability between different healthcare platforms using a smart edge gateway. Fortino *et al.* [12] proposed a framework *INTER-IoT*, a layer-wise architecture in both hardware and software layers to enable interoperability between different IoT layers and demonstrated the use-cases in logistics and healthcare. Wattana *et al.* [13] proposed blockchain-based technology to enable interoperability between different IoT services.
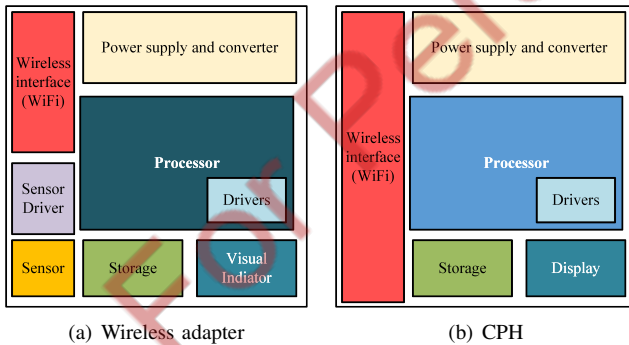

(a) Wireless adapter   (b) CPH

Fig. 3: Components of our implemented adapter and CPH.

Device-based interoperability aims at providing device-to-device communication, with scalable solutions. Multiple communication interfaces in devices such as Bluetooth, Zigbee, and WiFi have been proposed to enable device interoperability [14] [15] [16]. Adesina *et al.* [17] proposed a gateway-based hybrid approach to enable syntactic interoperability in IoT environment. Kotstein *et al.* [18] proposed a reinforcement learning to enable semantic interoperability in an IoT system with HTTP REST services.

A. Synthesis

The existing systems incorporate different forms of interoperability in various application domains. However, the systems are dependent on predefined ontologies and sensor information. Some of the systems are dependent on Internet connectivity to download system files and drivers for the devices. Additionally, all existing vendors do not practice the standard data formats. Hence, we propose and implement HeDI, which employs a wireless interoperable sensor adapter to introduce device interoperability in an in-home remote healthcare monitoring system.

III. SYSTEM MODEL

The system consists of three different units: 1) Wireless Sensor Adapter, 2) CPH, and 3) Remote server. The sensor adapter consists of a sensor attached to a WiFi-enabled controller board. The CPH encloses a WiFi-enabled processor board with a local storage unit. Fig. 3 shows the components of a wireless sensor adapter and CPH. The CPH creates an access point through which it receives the sensor data. In the star network configuration, each sensor adapter connects directly to CPH and transmits the sensor data. Mesh network configuration allows the sensor adapters to transmit the sensor data in the mesh network through multiple hops. The sensor adapter in the range of CPH eventually transmits the data to CPH. CPH collects the data from the connected sensor adapters, processes the data according to the proposed IP-based mapping scheme, and forwards it to the remote server. The CPH connects to a WiFi network to connect to the remote server through the Internet. Both traditional data transmission protocols, as well as IoT compliant light-weight protocols, can be used at the CPH to forward the received data to the remote server. In this work, we focus on the functioning of the sensor adapter and the CPH and discuss in details. Fig. 2 shows the implemented interoperable wireless sensor adapter with ECG, pulse, and temperature sensors connected to it. Table I shows a comparison of our implemented work with some of the existing similar systems and schemes.

A. Communication Architecture

The set of wireless adapters is denoted by $A = \{A_1, A_2, A_3, \ldots A_n\}$, each assigned a different data rate denoted by set $R = \{R_1, R_2, R_3, \ldots R_n\}$ where $n \in Z^+$ is the maximum number of adapters that can be connected to CPH. β is the total bandwidth allocated by CPH for the adapters to connect. We consider η number of channels for data transmission by the adapters. The maximum allowable data rate of all the adapters, when combined, is given as:

$$\Delta_A = \eta \cdot \sum_{i=1}^{n} R_i, \quad \Delta_A \leq \beta \qquad (3)$$

Let k number of adapters be connected to CPH at time instant t. The combined configured data rate is given as

$$D(t) = \eta \cdot \sum_{i=1}^{k} A_i(R_i) \quad \leq \Delta_A \qquad (4)$$

TABLE I: Comparison of the proposed architecture with the existing works.

Work	Monitoring Parameters	Device Heterogeneity (Sensor Types)	Flexibility		Addressed Interoperability	PDR	References
			Mode of Sensing	Max. no. of sensors allowed			
SDN-based WBAN for patient monitoring	Physiological	Undefined	wireless	Fixed	No	0.7	Ahmed *et al.* [19]
Remote health monitoring	Physiological	Pulse	Wireless Sensors	Fixed	No	0.87	Kharel *et al.* [20]
Patient monitoring using IoT	Physiological	Pulse Oximeter	Wireless	Fixed	No	0.89	Akkaş *et al.* [21]
Remote health monitoring	Physiological	Pulse (on demand)	Wearable	8(Bluetooth)	No	0.98	Al-Khafajiy *et al.* [22]
Proposed Work	Physiological	Temp, ECG, Pulse, and others (heterogeneous, on demand)	Wearable	250 (WiFi Standard, dynamic)	Yes	Mesh=0.98, Star= 0.92	–

where $A_i(R_i)$ denotes the configured data rate of the ith adapter. We define a bandwidth utilization ratio BR_U, which shows the actual bandwidth being used by the adapters all together from the allocated maximum allowable data rate. The difference in the two values is due to the changing number of adapters connected to CPH at an instant.

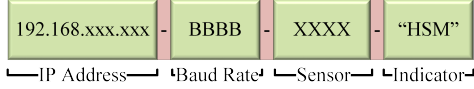$$BR_U = \frac{D(t)}{\Delta_A}, \quad \Delta_A > 0 \quad (5)$$

Fig. 4: Format of handshake packet.

1) Delay: The system encounters a communication delay δ when multiple adapters are connected to CPH. This delay is represented as a function of the number of connected adapters and their combined data rate, $\delta \propto n, \beta, R$. The transmission delay is the ratio of the total data generated at the adapter to the combined data rate of the adapter.

$$\delta_{trans} = \frac{1}{\eta} \cdot \frac{D(t) \cdot t_s}{\sum_{i=1}^{k} R_i} \quad (6)$$

Here t_s is the transmission time for the connected adapters. We calculate the propagation delay between the adapters and CPH as the ratio of the distance between adapter and CPH and the transmission speed between them given as $\delta_{prop} = \frac{l_i}{c_w}$ Here, c_w is the maximum transmission speed through the adapter's wireless interface, and l_i is the distance between the adapter and CPH. The mesh network incurs an additional delay due to a multi-hop path for data transmission, termed as the hop delay. Let δ_{hop} be the total delay in the mesh network till the penultimate sensor adapter which connected to CPH.

$$\delta_{hop} = \sum_{i,j=1}^{(n-1)} \frac{d_{i,j}}{s_t^i} \quad (7)$$

where $d_{i,j}$ is the distance in meters between the adapters A_i and A_j in the mesh network and s_t^i is the speed of data transmission of A_i. Let L_{queue} be the length of the queue for CPH. We calculate the queuing delay as the product of the

queue length and the transmission delay δ_{trans}.

$$\delta_{queue} = L_{queue} \times \left(\frac{D(t) \cdot t_s}{\sum_{i=1}^{k} R_i} \right) \quad (8)$$

The data is processed at CPH before forwarding it to the remote server. The processing at CPH includes the detection of the sensor from its IP and the data previously logged in the log file during information handshaking. Let t_{proc} be the processing time required for processing a unit bit of data. We calculate the total time required to process the data received by CPH from the connected adapters as

$$\delta_{proc} = t_{proc} \times \eta \cdot \sum_{i=1}^{k} R_i \times t_s \quad (9)$$

The total delay of the system is calculated as the sum of the transmission delay, propagation delay, hop delay, processing delay, and queuing delay.

$$\delta_{tot} = \delta_{prop} + \delta_{trans} + \delta_{hop} + \delta_{proc} + \delta_{queue}$$
$$= \left(t_{proc} \times \eta \cdot \sum_{i=1}^{k} R_i + \frac{1}{\eta} \cdot \frac{D(t)}{\sum_{i=1}^{k} R_i} (1 + L_{queue}) \right) \times$$
$$t_s + \frac{l_i}{c} + \sum_{i,j=1}^{(n-1)} \frac{d_{i,j}}{s_t^i} \quad (10)$$

It is to be noted that the hop delay for star network configuration is practically zero as the adapters transmit the data directly to CPH.
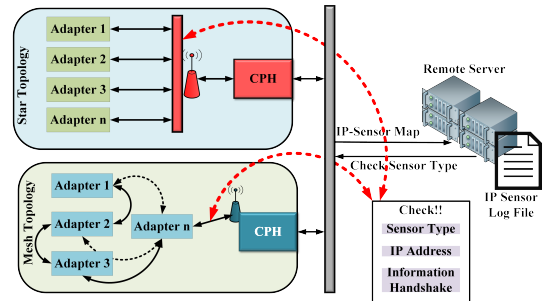

Fig. 5: An overview of the IP-sensor mapping at CPH.

2) Average Throughput: We calculate the average throughput between the connected adapters and CPH as a function

of the combined data generated at the adapters and the SNR values, using Shannon's capacity formula.

$$Throughput_{avg} = \frac{1}{k} \sum_{i=1}^{k} (D(t) \times \log_2(1 + SNR_i)) \quad (11)$$

Considering signal level $\mathbb{S}$ (mV) and noise level N (mV), $SNR = 20 log \frac{\mathbb{S}}{N}$ which can also be represented as $RSSI - N$.

3) Packet Delivery Ratio: The packet delivery ratio PDR_{CPH} is the ratio of successfully received data packets by CPH to the total number of transmitted data packets by the connected adapters. The PDR_{CPH} is dependent on the data rate of each adapter and its distance from CPH. Each adapter transmission experiences noise due to the other $k-1$ adapters transmitting to the same CPH. The distance between adapters and CPH reduces signal strength. Considering the Signal to Noise ratio, SNR, we represent the PDR_{CPH} as a function of the SNR_i and R_i of each adapter:

$$PDR_{CPH} = \frac{\sum_{i=1}^{k} \left(t_s \cdot R_i \cdot \log_2(1 + SNR_i) \right)}{\sum_{i=1}^{k} R_i \cdot t_s} \quad (12)$$

where $R_i \cdot \log_2(1 + SNR_i)$ is the effective data rate. We normalize the SNR_i values using the unit-less conversion of SNR values as shown in Equation (13).

$$SNR_i = 10^{SNR_{db}/10} \quad (13)$$

Let β_{CPH} be the bandwidth allocated to CPH for data transmission. The R_{CPH} is the data rate of CPH such that

$$D(t) \leq R_{CPH} \leq \beta_{CPH} \quad (14)$$

B. IP-based Device Mapping

When the sensor adapter connects to CPH's access point, CPH assigns an IP address to the adapter. Next, the system performs initial information handshaking between the adapter and CPH. During the handshaking, the sensor adapter transmits information about the IP address, baud rate, and the type of connected sensor to CPH in the form of an information packet (HIP) shown in Fig. 4. An indicator bit, In, identifies whether the received packet is an information packet or a sensor data packet. The sensor adapter adds the indicator at the beginning of each packet before forwarding it to CPH.

CPH stores the IP address of the sensor adapter, and the corresponding sensor type attached, in an IP-Sensor log file (ISL_f) and sends an acknowledgment to the sensor adapter. Upon receiving the acknowledgment, the adapter starts transmitting the sensor data to CPH, which forwards it to a remote server. Fig. 5 shows an overview of the information flow in the implemented system.

Every time a sensor adapter connects to CPH, the ISL_f is scanned to check the type of sensor attached to the sensor adapter. CPH adds a new entry if there is no existing entry of the IP address in ISL_f. If the entry for the received IP address already exists, CPH updates the ISL_f with the latest information. The local IP-based mapping is used to identify the type of sensor and segregate the data received simultaneously from multiple sensor adapters.

Algorithm 1 IPMaD: IP-based mapping at adapter

1: **if** A_i connected to CPH **then**
2:     Send HIP and wait for acknowledgment
3:     **if** Acknowledgment received **then**
4:         **if** Star network **then**
5:             Send sensor data $\rightarrow$ CPH
6:         **end if**
7:         **if** Mesh network **then**
8:             Broadcast sensor data $\rightarrow$ network
9:         **end if**
10:     **else** Resend acknowledgement
11:     **end if**
12: **end if**

Algorithm 2 IPMaC: IP-based mapping at CPH

1: **for** Connected A_i **do**
2:     Receive HIP
3:     Verify ISL_f
4:     **if** Device already found **then**
5:         Update ISL_f
6:     **else** Add IP-Sensor mapping $\rightarrow ISL_f$
7:     **end if**
8:     Send acknowledgment
9:     Receive sensor data
10:     Send data to remote server based on IP-Sensor mapping
11: **end for**

The IPMaD (Algorithm 1) is implemented in the sensor adapter to enable communication between the adapter and CPH. IPMaD acts as a client and waits to connect to CPH's access point. Once connected, the sensor adapter starts transmitting the HIP to the CPH until it receives an acknowledgment. Once the acknowledgment arrives, the sensor adapter starts sending the sensor data to CPH. Similarly, the IPMaC (Algorithm 2) is implemented at CPH and acts as a server. Whenever the CPH receives a data packet, it looks for the In bit in the message to verify if it is a HIP. Once verified, it sends an acknowledgment to the sensor adapter and logs the adapter information in the local ISL_f. If the received packet is a sensor data packet, CPH scans the ISL_f and segregates the data as per the sensor type associated with the IP address. CPH then forwards the segregated data to the remote server. The IP-based data mapping allows the system to have homogeneous sensors connected simultaneously to CPH.

C. Network Topology

We use two different network topologies (star and mesh) in our system. In star topology, the adapters are directly connected to CPH. In a mesh topology, the adapters dynamically form a mesh network. The adapter nearest to CPH forwards the data from the mesh network. The star topology incurs less transmission delay due to the direct connection between the CPH and adapters. Whereas, the mesh network ensures minimum packet loss with permissible delay due to the multi-hop network. A long-range monitoring environment can exploit the mesh topology to enable adapters' communication with CPH, which may not be possible in the star network. Although there are many other network topologies such as ring, tree, and hybrid network topologies that can be implemented using the proposed system, the utility of such topologies will depend on the scenario. The choice of network topologies will depend on the placement of the sensor adapters. As our system is based on wireless wearable units, the bus topology, which is wired,
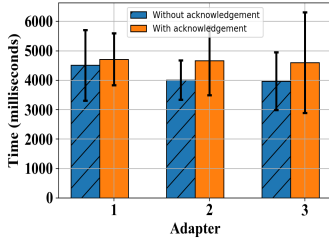
Fig. 6: Time for successful connection establishment and acknowledgment between sensor adapter and CPH.
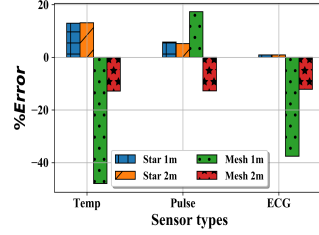

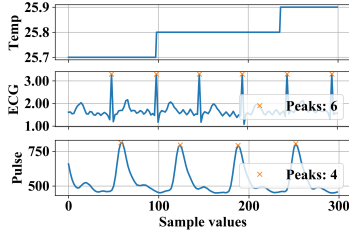Fig. 7: Evaluation of data delivery with multiple sensor adapters connected to CPH.

Fig. 8: Sensor data received at CPH from the 3 sensor adapters

is not considered. A tree topology can be formed by placing the CPH as the root and then extending the branch networks by carefully placing the adapters. Similarly, a ring topology can be achieved by placing the adapters in a linear formation and ensuring that each adapter in the network is uniquely connected to exactly two adapters. However, the star and mesh are commonly used topologies, especially in Wireless Body Area Network (WBAN), which our system intends to achieve.

IV. PERFORMANCE EVALUATION

We implemented the proposed system in real-time in a laboratory environment. The system is implemented and tested for three different sensors –Temperature, Pulse, and a 3-lead ECG. We deployed a bare basic system implementation for evaluating the proof-of-concept proposed in this work. We used a single WiFi channel (default) for communication and a UDP-based socket for data transmission between the adapter and the CPH. However, more advanced protocols such as those based on TCP/IP, MQTT and CoAP can also be used for this communication. The choice of these protocols can be easily customized based on the application requirements. We used a Raspberry pi 3 model B to implement CPH, which has a 1.2 GHz quad-core ARMv8 processor with 1 GB RAM and 802.11n wireless LAN. During data transmission, the CPH is placed in a fixed location, and powered through a regular wall socket using a 5V AC-to-DC adapter. The experiment used two different network topologies – star and mesh. We set the baud rate of adapters at 4800 for the experiments. We record a 60 second data from each of the adapters in the network. We repeat the experiment for a distance of 1m and 2m between CPH and adapters. The data set used in our work has been generated in real-time with the implemented system. The data has been manually and visually validated.

We have used multiple subjects to check the consistency of the incoming data. The primary attributes of our data set are- sensor value, duration of data sent, duration of data received. Other attributes such as number of packets, data size, and delay are derived from the three primary attributes

A. Connection Time of Sensor Adapters

Fig. 6 shows the connection time for each adapter connected in consecutive order to CPH, wirelessly. We consider two cases for the connection time in adapters- 1) time taken to connect to CPH and 2) time taken to complete the initial information handshaking process. The connection time for the first adapter is higher than the next two adapters by an average time of $100ms$. We attribute this behavior to the hardware scanning process for the network during the initial setups. An average increase of $488ms$ is observed in the acknowledgment time with the increasing number of adapters connected to CPH. The increased acknowledgment time is due to multiple simultaneous requests from adapters to CPH after handshaking. The overall system performance shows average connection delay in the range of milliseconds, mostly due to the one-time processing within the sensor adapter during start-up.
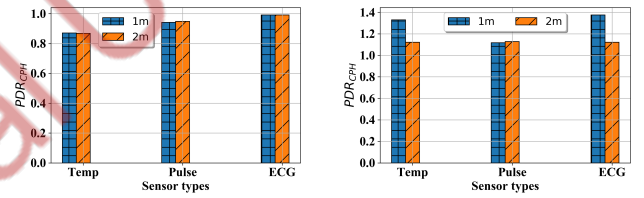
(a) PDR at CPH in star topology

(b) PDR at CPH in mesh topology

Fig. 9: PDR at CPH for 60 seconds of generated data in star and mesh network configuration

B. Packet Delivery Ratio

We evaluate the variation in PDR_{CPH} with varying distance between the adapters and CPH. The variation is recorded for different sensors in star and mesh network topology for 60 seconds, as shown in Fig. 9. Fig.9(a) shows the PDR_{CPH} of the system in a star network configuration. We observe a minimum PDR_{CPH} of 0.86 and a maximum PDR_{CPH} of 0.99 in the star network. An average drop of 0.01 in PDR_{CPH} is observed when the distance increases to $2m$. The system works well and allows mobility for the user or patient within the tested operational range. Fig.9(b) shows the PDR_{CPH} of the system in a mesh network configuration. In some instances, the size of data delivered to CPH exceeds by approximately 2108 bytes for 59000 bytes of data generated at the sensor adapter due to multiple transmission of the same data packets in the mesh by multiple sensor adapters. While this phenomenon will increase the chances of higher successful deliveries, it also creates undesirable network traffic resulting in a decrease in true PDR_{CPH}. A packet sequencing mechanism can be implemented at the adapter to avoid duplicate data transmissions.

## C. Quality of the Received Data

The temperature and pulse data have simple waveforms and exhibit small variations over time, making them more stable. The transmission frequency of such data can be reduced to allow the transmission of complex time-critical data. On the contrary, ECG has a complex waveform and is more time-sensitive in nature. An ECG signal is a complex composition of 3 different types of waveforms followed as the P wave, QRS complex, and S wave. The duration of each ECG complex is approximately 0.7 seconds. Such time-critical data must be transmitted with high frequency and accuracy to avoid any data loss. We plot the ECG, pulse, and temperature data received at CPH without using any filters in Fig.8 to study the variations in the signals and the extent of information loss. Fig. 8 shows a sub-section of 300 data points of the 60 seconds of the received ECG, pulse, and temperature values. Fig.7 shows the error in data transmission concerning lost packets for the two network configurations. The system exhibits a maximum error of 17.3%. The star configuration has an average data loss of 2500 bytes. In mesh configuration, the number of packets received at CPH exceeds the actual size of data generated by an average of 2650 bytes. The negative error % in Fig.7 signifies the excess packets received due to redundant data packets from the multi-hop mesh network. On the contrary, star configuration establishes a direct connection between adapters and CPH, with no duplicate transmission.

D. Delay at CPH

We evaluate the delay in the received data at CPH for both the network topologies, as shown in Fig.10. The 3 adapters generate 59000 bytes of data, where the mesh network receives a total of 61650 bytes and star network receives 5650 bytes of data. The delay in the network increases with the increasing number of adapters connected to the network. The mesh network exhibits a maximum delay when 3 adapters are connected to the network, while the star network gives minimum delay when 1 adapter is connected to the network. Star topology performs significantly better than the mesh topology in terms of delay incurred at CPH. The delay in the mesh network is due to multiple hops between the transmitting node and CPH. With the increasing number of adapters in the network, the hop count for data transmission increases, increasing delay at CPH from 2 seconds for one adapter to 136 seconds for three adapters. In the star network, the adapters are directly connected to CPH, or we can say that it is a one-hop connection. Hence we infer that star network configuration should be used for time-critical applications to minimize δ_{tot}.

E. Evaluation of Network Topologies

We implemented and compared our remote healthcare monitoring system for two different network configurations. Fig.11 shows the comparison of the configurations concerning delay and number of connected adapters in the network. The star configuration achieves a minimum delay of 0.056 seconds and a maximum delay of 1.49 seconds in data transmission
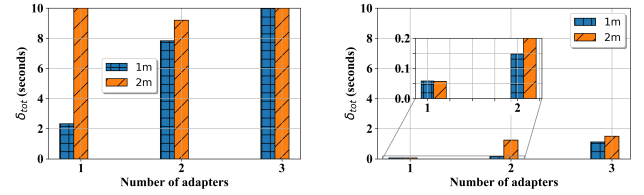
(a) Delay at CPH in mesh topology (b) Delay at CPH in star topology

Fig. 10: Delay in reception of data at CPH for 60 seconds of generated data

due to the direct connection of sensor adapters to CPH. The configuration is suitable for real-time monitoring and assessment of patient's health. Star network is useful in situations where critical and time-bound monitoring is required. However, the need for a direct connection between CPH and sensor adapters decreases the range of CPH connectivity. This means that the mobility of a patient is restricted within the direct range of CPH. Patients with restricted mobility and fluctuating physiological conditions can be monitored using the star network configuration.

Mesh network configuration has a higher packet delivery ratio with a maximum of 1.37 and a minimum of 1.11, ensuring high accuracy. A packet delivery ratio greater than one signifies that more packets get delivered than the actual generated. This behavior is attributed to the mesh network's characteristic of enhancing packet redundancies in the network to ensure reliable data delivery. However, the mesh configuration also introduces a significant average delay of 30 seconds and a maximum delay of 136 seconds due to multi-hop data transmission. The mesh network can be used to monitor a patient's physiological parameters over long periods of observation. Mesh network also provides the patient with higher mobility due to its ability to network over multiple hop communication links.

F. Scalability of the System

We evaluate the scalability of the proposed work based on the following features of the proposed system:

- The proposed system uses wearable sensor adapters, which easily integrate into the system without making any changes to the existing hardware. When new physiological parameters need to be monitored in a patient, new sensor adapters can be integrated with the existing system without changing the existing hardware.
- The system uses WiFi to connect the wearable adapters to the CPH. WiFi allows a maximum of 250 devices to be connected simultaneously to the network. This allows the system to connect a huge number of wearables. This feature is especially harnessed by the star topology, where all the adapters connect directly through the one-hop distance to CPH.
- The mesh network configuration increases the range of the wearables adapters through its multi-hop data transmission to the CPH. This allows for long-range data transmission between the adapters and CPH. The network

of adapters can be increased indefinitely until the system delay becomes infeasible.

Fig. 11: Comparison of delay in star and mesh configurations with varying number of adapters (A)

V. Conclusion

In this paper, we proposed and implemented HeDI, which uses our developed interoperable sensor adapter for a portable in-home wireless healthcare monitoring system with a central processing hub (CPH) and multiple interoperable sensor adapters. The wireless adapters have a low form factor and provide the freedom of mobility for remote health monitoring within the evaluated ranges. We implemented an IP mapping-based algorithm, IPMaC for CPH and IPMaD for the adapter to incorporate interoperability. We implemented and evaluated the system for two different network configurations – star and mesh and characterized the system in terms of its basic network and device parameters.

The implemented system exhibits reliability with its wireless interoperable sensor adapters in both the implemented networks with minimum PDR of 0.86 with 3 adapters connected to the network with high accuracy despite the packet loss. The mesh configuration allows each sensor adapters in the network to act as transmission nodes. Mesh network enables a sensor adapter to send its data to longer distances through intermediate adapters. Additionally, the connection traffic at CPH is also reduced. The scalability of the system is evident from the high PDR values and low percentage error. Our implemented interoperable adapter enables dynamic integration of new sensors in the system.

The star and mesh networks have their limitations. In future, star network can be supported with robust algorithms to ensure a higher PDR and minimize network traffic.

VI. Acknowledgment

The authors would like to thank Sensordrops Networks Pvt. Ltd. for providing the platfrom and sensor nodes.

References

[1] A. Triantafyllou, P. Sarigiannidis, and T. D. Lagkas, "Network protocols, schemes, and mechanisms for internet of things (iot): Features, open challenges, and trends," *Wireless communications and mobile computing*, vol. 2018, 2018.

[2] M. Noura, M. Atiquzzaman, and M. Gaedke, "Interoperability in internet of things: Taxonomies and open challenges," *Mobile Networks and Applications*, vol. 24, no. 3, pp. 796–809, 2019.

[3] F. Yang, N. Matthys, R. Bachiller, S. Michiels, W. Joosen, and D. Hughes, "μ pnp: plug and play peripherals for the internet of things," in *Proceedings of the tenth European conference on computer systems*. ACM, 2015, p. 25.

[4] N. Matthys, F. Yang, W. Daniels, W. Joosen, and D. Hughes, "Demonstration of micropnp: the zero-configuration wireless sensing and actuation platform," in *2016 13th Annual IEEE International Conference on Sensing, Communication, and Networking (SECON)*. IEEE, 2016, pp. 1–2.

[5] H. Derhamy, J. Eliasson, and J. Delsing, "Iot interoperability—on-demand and low latency transparent multiprotocol translator," *IEEE Internet of Things Journal*, vol. 4, no. 5, pp. 1754–1763, 2017.

[6] S. Yang and R. Wei, "Tabdoc approach: an information fusion method to implement semantic interoperability between iot devices and users," *IEEE Internet of Things Journal*, 2018.

[7] S. Raj and K. C. Ray, "A personalized point-of-care platform for real-time ecg monitoring," *IEEE Transactions on Consumer Electronics*, vol. 64, no. 4, pp. 452–460, 2018.

[8] M. Chen and Y. Hao, "Label-less learning for emotion cognition," *IEEE transactions on neural networks and learning systems*, 2019.

[9] M. Chen, Y. Jiang, N. Guizani, J. Zhou, G. Tao, J. Yin, and K. Hwang, "Living with i-fabric: Smart living powered by intelligent fabric and deep analytics," *IEEE Network*, 2020.

[10] M. Chen, Y. Cao, R. Wang, Y. Li, D. Wu, and Z. Liu, "Deepfocus: Deep encoding brainwaves and emotions with multi-scenario behavior analytics for human attention enhancement," *IEEE Network*, vol. 33, no. 6, pp. 70–77, 2019.

[11] T. Sigwele, Y. F. Hu, M. Ali, J. Hou, M. Susanto, and H. Fitriawan, "An intelligent edge computing based semantic gateway for healthcare systems interoperability and collaboration," in *2018 IEEE 6th International Conference on Future Internet of Things and Cloud (FiCloud)*. IEEE, 2018, pp. 370–376.

[12] G. Fortino, C. Savaglio, C. E. Palau, J. S. de Puga, M. Ganzha, M. Paprzycki, M. Montesinos, A. Liotta, and M. Llop, "Towards multi-layer interoperability of heterogeneous iot platforms: the inter-iot approach," in *Integration, Interconnection, and Interoperability of IoT Systems*. Springer, 2018, pp. 199–232.

[13] W. Viriyasitavat, L. Da Xu, Z. Bi, and A. Sapsomboon, "New blockchain-based architecture for service interoperations in internet of things," *IEEE Transactions on Computational Social Systems*, vol. 6, no. 4, pp. 739–748, 2019.

[14] P. Karthika, R. G. Babu, and P. Karthik, "Fog computing using interoperability and iot security issues in health care," in *Micro-Electronics and Telecommunication Engineering*. Springer, 2020, pp. 97–105.

[15] M. Clarke, J. de Folter, V. Verma, and H. Gokalp, "Interoperable end-to-end remote patient monitoring platform based on ieee 11073 phd and zigbee health care profile," *IEEE Transactions on Biomedical Engineering*, vol. 65, no. 5, pp. 1014–1025, May 2018.

[16] P. Pace, G. Aloi, R. Gravina, G. Caliciuri, G. Fortino, and A. Liotta, "An edge-based architecture to support efficient applications for healthcare industry 4.0," *IEEE Transactions on Industrial Informatics*, vol. 15, no. 1, pp. 481–489, 2019.

[17] T. Adesina and O. Osasona, "A novel cognitive iot gateway framework: Towards a holistic approach to iot interoperability," in *2019 IEEE 5th World Forum on Internet of Things (WF-IoT)*. IEEE, 2019, pp. 53–58.

[18] S. Kotstein and C. Decker, "Reinforcement learning for iot interoperability," in *2019 IEEE International Conference on Software Architecture Companion (ICSA-C)*. IEEE, 2019, pp. 11–18.

[19] O. Ahmed, F. Ren, A. Hawbani, and Y. Al-Sharabi, "Energy optimized congestion control-based temperature aware routing algorithm for software defined wireless body area networks," *IEEE Access*, vol. 8, pp. 41 085–41 099, 2020.

[20] J. Kharel, H. T. Reda, and S. Y. Shin, "Fog computing-based smart health monitoring system deploying lora wireless communication," *IETE Technical Review*, vol. 36, no. 1, pp. 69–82, 2019.

[21] M. A. Akkaş, R. SOKULLU, and H. E. Çetin, "Healthcare and patient monitoring using iot," *Internet of Things*, p. 100173, 2020.

[22] M. Al-Khafajiy, T. Baker, C. Chalmers, M. Asim, H. Kolivand, M. Fahim, and A. Waraich, "Remote health monitoring of elderly through wearable sensors," *Multimedia Tools and Applications*, vol. 78, no. 17, pp. 24 681–24 706, 2019.